Single-cycle-pulse generation in a coherently mode-locked laser with an ultrashort cavity

Rostislav Arkhipov ,[1] Mikhail Arkhipov,[1] Anton Pakhomov ,[1] Ihar Babushkin,[2,3,4] and Nikolay Rosanov[1,5]
[1]*St. Petersburg State University, Universitetskaya nab. 7/9, St. Petersburg 199034, Russia*
[2]*Leibniz University Hannover, Institute of Quantum Optics, Welfengarten 1, 30167 Hannover, Germany*
[3]*Cluster of Excellence PhoenixD (Photonics, Optics, and Engineering - Innovation Across Disciplines), Welfengarten 1, 30167 Hannover, Germany*
[4]*Max Born Institute, Max-Born-Strasse 2a, Berlin 10117, Germany*
[5]*Ioffe Institute, Politekhnicheskaya str. 26, St. Petersburg 194021, Russia*

(Received 30 October 2021; revised 30 December 2021; accepted 5 January 2022; published 27 January 2022; corrected 31 January 2022)

We theoretically investigate the possibility of a passive mode-locking regime in a two-section laser with an ultrashort cavity of the length around ten wavelengths of the medium resonant transition or even less. It is shown that such a regime is enabled through the coherent mode-locking phenomena arising due to the self-induced transparency when the gain and absorption bandwidths do not impose any restrictions on the duration of the generated pulse. Under such conditions, a laser with an ultrashort cavity could produce output pulses with the terahertz (THz) repetition rate and the duration up to a single optical cycle. Moreover, several scaling rules were derived, which allow for further shortening of the output pulse duration with the respective scaling of the media parameters.

DOI: 10.1103/PhysRevA.105.013526

I. INTRODUCTION

Mode-locking in lasers represents one of the most common ways to generate ultrashort optical pulses [1–4]. This regime relies on the nonlinear properties of an absorber, which is placed inside a laser cavity and gets saturated for the large intensity of the generated pulses thus reducing the pulse absorption [3,4]. In this case, the mode-locking regime arises due to the gain/absorber incoherent saturation. Interaction of the laser pulse with gain and absorbing medium is incoherent when the Rabi frequency $\Omega_R = d_{12}E_0/\hbar$ is smaller than the inverse medium polarization relaxation time $1/T_2$, where d_{12} is the transition dipole moment of the intracavity medium, E_0 is the electric field amplitude, and $\hbar$ is the reduced Planck constant. At the same time, the achievable pulse duration in conventional passively mode-locked lasers is limited by the relaxation time T_2: $\tau_p > T_2$.

The nonlinear modulation of the cavity losses can be also achieved by the almost instantaneous Kerr-lense self-focusing of a beam in a transparent intracavity optical element. This approach has made it possible to produce few-cycle pulses in Ti:sapphire lasers [5]. At the same time, a saturable-absorber-based technique has been actively used for mode-locking in fiber lasers [6–8]. It allows picosecond and femtosecond pulse generation in such devices. However, the pulse duration is also limited by the polarization relaxation time of the lasing medium T_2.

Such restrictions on the gain/absorption bandwidth do not arise when the light-matter interaction in the gain and absorber is coherent, i.e., $\Omega_R > 1/T_2$, so that the pulse duration is less than the polarization relaxation time T_2: $\tau_p < T_2$ [9,10]. In this case, gain and absorber medium can not remain in the saturated state, because the coherent Rabi oscillations of the atomic inversion occur over the pulse duration. The mode-locking phenomenon provided by the coherent light-matter interaction is called the coherent mode-locking (or self-induced transparency mode-locking) and was studied theoretically in Refs. [11–21].

According to the original idea of coherent mode-locking proposed in Ref. [11], an ultrashort pulse produced through the coherent mode-locking propagates in the absorber without losses due to the self-induced transparency phenomenon (SIT). SIT was studied theoretically and observed experimentally in the pioneering work of McCall and Hahn [22,23]. It arises when a short high-power pulse of the duration shorter than the medium coherence relaxation time T_2 resonantly propagates in an absorbing medium.

The leading edge of the pulse transfers medium from the ground state to the excited state due to the stimulated absorption, while at the trailing the medium returns back to the ground state due to the stimulated emission. The area of this pulse calculated through the pulse envelope

$$\Theta = \frac{d_{12}}{\hbar}\int_{-\infty}^{+\infty} \mathcal{E}(t)dt,$$

which is equal to 2π, therefore such a pulse is called 2π pulse. At the same time inside the gain section, the so-called π pulse arises having the pulse area $\Theta = \pi$ [10,11]. Such a π pulse transfers the gain medium from the excited state to the ground state extracting most of the energy stored in the gain medium.

SIT phenomenon as well as coherent Rabi oscillations were studied both theoretically and experimentally in plenty of media, such as gases, solids, and quantum dots [9,10,24–29]. In spite of the huge amount of experimental observations in various media, application of SIT for mode-locking in lasers was not considered for a long time in the literature [30].

In the case of coherent mode-locking, the gain and absorption bandwidths do not impose any limitations on the duration of the generated pulse anymore with respect to the standard passively mode-locked lasers with saturable absorbers [11–20]. In this case, the ultrashort pulse generation in a narrowband medium becomes possible. The experimental investigation of coherent mode-locking was not carried out for a long time mainly because of the common point of view that narrowband gain and absorbing media can not support an ultra-short pulse propagation [30].

In a single-section laser, first experimental observation of the coherent mode-locking with π pulses was made by Fox and Smith in Ref. [31] already at the beginning of the laser era. These were nanosecond-scale pulses operated in a meter-long cavity. The experimental observation of the coherent mode-locking regime in a two-section laser was first reported fairly recently. Namely, in Refs. [32,33], the mode-locking based on 0π-pulse formation in a dye laser with a coherent absorber cell has been reported. Mode-locking based on the self-induced transparency and 2π-pulse formation in a coherent absorber was experimentally observed for the first time in a Ti:sapphire laser [34–36] with a coherent absorber section placed inside the laser cavity. In all experiments mentioned above, long multicycle pulses were obtained and long cavities were used.

The coherent mode-locking regime is of interest for the generation of single-cycle pulses, as it was shown earlier in ring-cavity lasers upon neglecting the relaxation processes in laser media during a single round-trip [16,17]. In practice, however, lasers typically have linear cavities, and the generation of femtosecond or attosecond pulses requires bulky setups [37]. Therefore it looks challenging to achieve the coherent mode-locking regime in an ultrashort cavity of the length below 1 mm in order to get a very high pulse repetition rate as well as possibly a short pulse duration.

We note that in such a short cavity the pulse duration can also constitute just a few optical cycles or even less, which is much shorter than the polarization relaxation times T_2 in the gain and absorber (the value of T_2 can be hundreds of femtoseconds in semiconductors and solids at room temperature). Thus the condition of $\tau_p < T_2$ can be easily satisfied using ultrashort cavities and the mode-locking arising in this case will be due to the coherent effects.

In this paper, we theoretically demonstrate the possibility of the coherent mode-locking regime in a linear-cavity laser with the cavity length around ten transition wavelengths, which allows producing near single-cycle pulses. We also derive several scaling rules for the full Maxwell-Bloch laser equations, meaning that for each generation regime obtained the further downscaling of the output pulse duration is possible provided that the parameters of all intracavity media are rescaled accordingly.

II. THE MODEL AND RESULTS

Theoretical studies of the passive mode-locking often apply significant simplifying assumptions. Among them are, for instance, the ring-cavity model with the unidirectional propagation of the radiation or the slowly varying envelope approximation (SVEA) and rotating-wave approximation (RWA), which are widely used when simulating coherent mode-locking [13–15,18–20].

Typically, however, lasers posses a linear cavity resulting in the existence of the counter-propagating waves inside the laser cavity, which affect the mode-locking by creating the population density gratings. Besides that, SVEA and RWA approximations become invalid when modeling the few-cycle pulses. Therefore we use the full system consisting of the one-dimensional wave equation for the electric field and the density matrix equation for a two-level medium to describe the coherent mode-locking regime. Moreover, we simulate the mirrors as finite-thickness metallic layers described by the standard Drude model [38]. The system of equations attain the form:

$$\frac{\partial^2 E(z,t)}{\partial z^2} - \frac{1}{c^2}\frac{\partial^2 E(z,t)}{\partial t^2} = \frac{4\pi}{c^2}\frac{\partial^2 P(z,t)}{\partial t^2}. \quad (1)$$

$$\frac{d\rho_{12}(z,t)}{dt} = -\frac{\rho_{12}(z,t)}{T_2} + i\omega_0\rho_{12}(z,t) - \frac{id_{12}}{\hbar}n(z,t)E(z,t), \quad (2)$$

$$\frac{d}{dt}n(z,t) = -\frac{n(z,t)-n_0}{T_1} + \frac{4d_{12}E(z,t)}{\hbar}\mathrm{Im}(\rho_{12}(z,t)), \quad (3)$$

$$P(z,t) = 2d_{12}N_0\mathrm{Re}\rho_{12}(z,t), \quad (4)$$

$$\ddot{x}(z,t) + \gamma\dot{x}(z,t) = \frac{e}{m}E(z,t), \quad (5)$$

$$P(z,t) = eN_{\mathrm{el}}x(z,t), \quad (6)$$

Here the following quantities are used: $E(z,t)$ is the linearly polarized electric field, c is the speed of light in vacuum, $P(z,t)$ is the induced polarization of the medium provided by the non-diagonal element of density matrix ρ_{12} and the volume density of particles N_0, ω_0 is the resonant frequency of the medium (the respective wavelength is $\lambda_0 = 2\pi c/\omega_0$), d_{12} is the transition dipole moment, n_0 is the equilibrium value of the population inversion without the driving electric field, $n = \rho_{11} - \rho_{22}$ is the population inversion between the ground and excited states (diagonal elements), $x(z,t)$ is the electron shift in the metal, N_{el} is the volume density of free electrons in the metal, γ is the damping rate of the free electrons, e and m are the electron charge and mass.

Equations (2) and (3) also include the coherence relaxation time T_2 and the inversion relaxation time T_1. The medium can be considered as absorbing or amplifying one depending on the sign of n_0. It should be noted that for an ultrashort laser cavity the dispersion of the host medium can be safely neglected. The system of equations (1)–(6) was solved numerically using the finite-difference time-domain method for the wave equation (1) and Runge-Kutta method for the equations (2)–(6). The basic scheme of the considered setup and the relative locations of the constitutive elements are shown in Fig. 1.

An example of the calculation demonstrating the appearance of the coherent mode-locking regime is presented in Fig. 2. The sizes are $\Delta_1 = \Delta_2 = 0.28$ μm, $L_{\mathrm{cav}} = 6.9$ μm, $Z_g = 0.7$ μm, $Z_a = 3.85$ μm, and $L_g = L_a = 2.45$ μm.

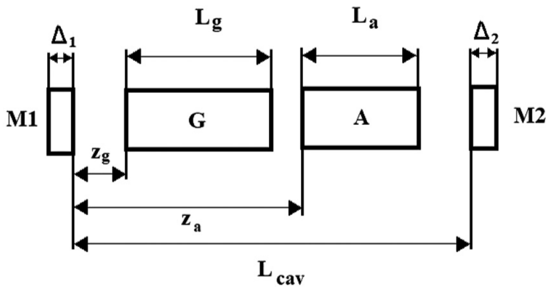

FIG. 1. The cavity arrangement: M_1 and M_2 are the metallic cavity mirrors, G and A are the gain and absorber media, respectively, Δ_1 and Δ_2 are the mirror thicknesses, L_{cav} is the distance between the mirrors, Z_g and Z_a are the distances from the left mirror to the gain and absorber sections, L_g and L_a are the lengths of the gain and absorber sections.

The parameters of the gain are $N_g = 1.5 \times 10^{21}$ cm^{-3}, $T_{1g} = 500$ fs, $T_{2g} = 10$ fs, and $d_g = 5$ D. The parameters of the absorber are $N_a = 2.5 \times 10^{20}$ cm^{-3}, $T_{1a} = 100$ fs, $T_{2a} = 10$ fs, and $d_a = 10$ D. The concentration of electrons in the metallic mirrors $N_{\text{el}} = 4 \times 10^{21}$ cm^{-3} and the damping rate is $\gamma = 10^{13}$ s^{-1}.

The regime of the coherent mode-locking turns out to be self-starting and therefore does not require any seed pulse to be injected into the cavity. It was verified at different initial radiation levels in the cavity, which were low at the beginning of the calculation.

The stroboscopic picture of the lasing pulses evolution leaving the cavity is shown in Fig. 2. The following technique was used to construct it. The calculation data, containing N values of the field strength at the exit from the resonator, were divided into successive fragments of the same length. It corresponds to the time that the pulse bypasses the resonator and has ΔN values. The number of these fragments is $K = N/\Delta N$. The matrix $(\Delta N \times K)$ was built where these fragments were placed. All fragments are displayed in the form of a three-dimensional dependence as shown in Fig. 2. Figures 3 and 4 show several fragments at the beginning and several fragments at the end of the calculation interval, while Fig. 5 shows the evolution of the field spectrum.

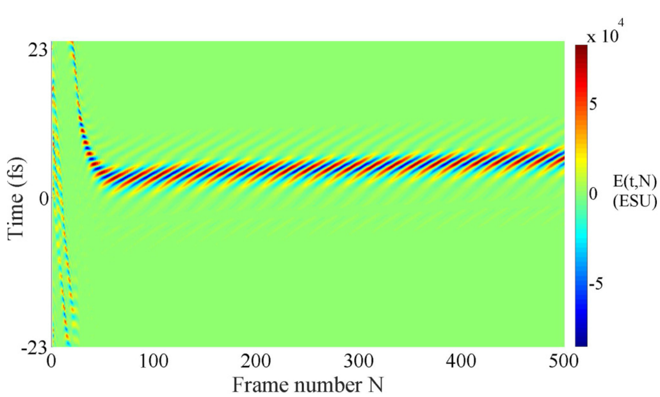

FIG. 2. The calculation results for the electric field inside an ultrashort-cavity laser under the coherent mode-locking regime. The cavity arrangement is shown in Fig. 1, the parameter values for the laser cavity as well as for the gain and absorber media are listed in the text.

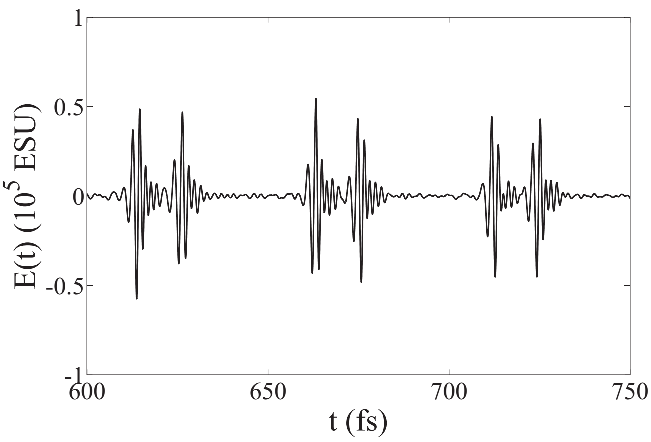

FIG. 3. A fragment of the temporal evolution of the electric field inside the ultrashort cavity from Fig. 2, corresponding to the transient stage of the pulse dynamics.

The transient process takes place at the initial stage and evolves to a stationary regime. Before the formation of a pulse of the self-induced transparency in the stationary regime, there are two coupled pulses in lasing in Fig. 3. At this stage, the spectrum has the characteristic dip at the transition frequency, since upon the transition from one pulse to another the phase changes by π. Both pulses form one 0π-pulse with zero area in Fig. 3. Then two pulses are transformed into one 2π pulse of the self-induced transparency in Fig. 4. The obtained 2π pulse in Fig. 4, which propagates in the cavity in a stable regime, appears to comprise just a single full optical cycle. A similar scenario of the stationary coherent mode-locking formation was observed experimentally [36] in the case of long pulses.

It is also important to address the achieved value of the pulse repetition rate. As one can see from Fig. 4, due to the ultrashort laser cavity the obtained pulse repetition rate constitutes roughly 20 THz, which largely exceeds the typical values in standard passively mode-locked lasers.

Figures 6 and 7 show the calculation results when the time T_{2a} in the absorber was increased. At absorber time

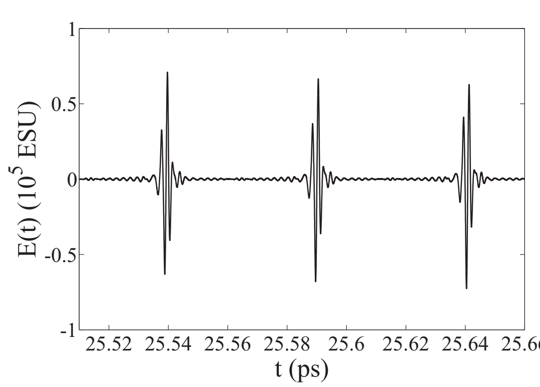

FIG. 4. A fragment of the temporal evolution of the electric field inside the ultrashort cavity from Fig. 2, demonstrating the stable regime of the coherent mode-locking.

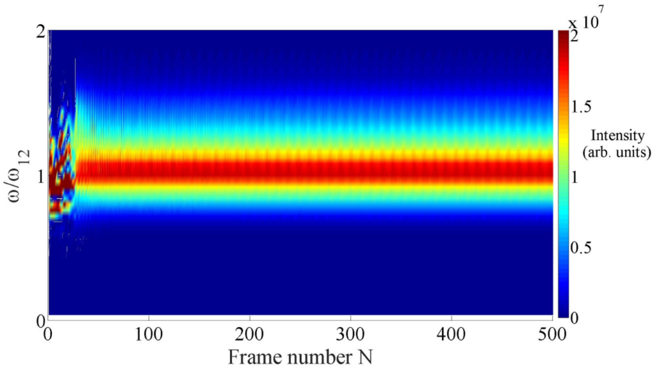

FIG. 5. The temporal evolution of the spectrum of the electric field inside the ultrashort cavity from Fig. 2.

$T_{2a} = 50$ fs in Fig. 6 the pulse moves up and down in the diagram. We observe a slow change in the repetition period of a single 2π pulse. In Fig. 7 at $T_{2a} = 100$ fs, the mode-locking regime disappears. The reason for the mode-locking disappearance lies in the appearance of population gratings, and polarization waves in the absorber, which hinders the pulse propagation. Polarization waves form the radiation, which interferes with the mode-locking pulse, changes its amplitude and reduces the pulse contrast. According to the calculation results, the longer time T_2 is the deeper the modulation of the population difference gratings is given. The grating produces the pulse backward scattering which destroys the mode-locking pulse up to its disappearance.

III. DISCUSSION AND POSSIBILITY OF EXPERIMENTAL REALIZATION

We should note the difference between our work and the previous ones. Earlier, the case of the unidirectional generation in the ring cavity laser was considered [16,17]. There, if all relaxation processes were terminated during the cavity round-trip time, the single-cycle pulse was obtained in the coherent mode-locking. Such a condition means that the relaxation times should be less than the cavity round-trip time, which imposes a very strong limitation on the laser geometry.

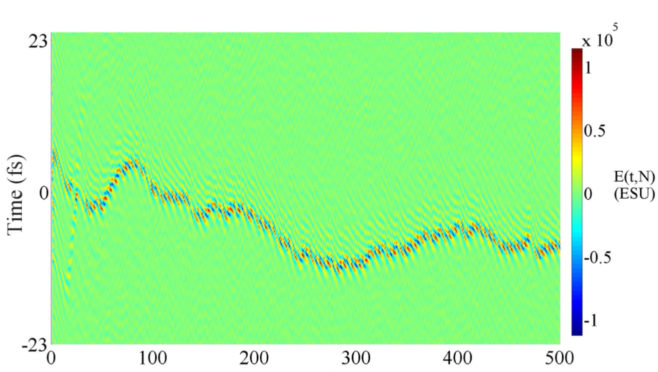

FIG. 6. Simulation results for the electric field inside an ultrashort-cavity laser under the coherent mode-locking regime for the larger value of the coherence relaxation time T_2 in the absorber: $T_{2a} = 50$ fs. Other parameters are the same as in Figs. 2–4.

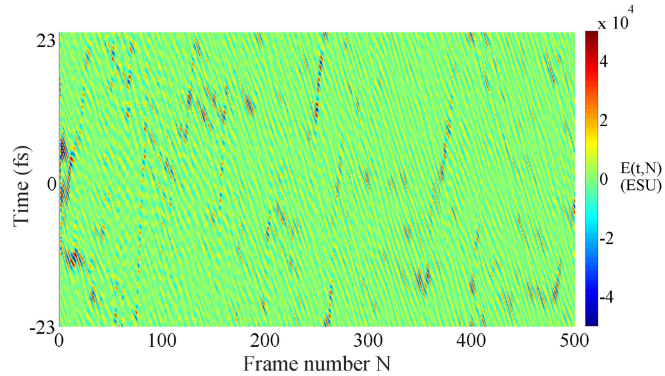

FIG. 7. Simulation results for the electric field inside an ultrashort-cavity laser under the coherent mode-locking regime for the larger value of the coherence relaxation time T_2 in the absorber: $T_{2a} = 100$ fs. Other parameters are the same as in Figs. 2–4.

In contrast, in our modeling of a two-section laser with a linear cavity, the relaxation times T_1 and T_2 were taken longer than the cavity round-trip time. Therefore the laser media contained residual population gratings and polarization waves. They arise during the counter-propagation of few-cycle pulses in the resonant media [39,40]. The polarization waves exist for the time T_2, while the population gratings exist during the time T_1. The larger T_2 is, the longer the lifetime of the polarization waves is. At the same time, the population gratings are caused by the interference of the induced polarization waves with the counter-propagating mode-locking pulse in the cavity. The deeper these gratings are, the more they spoil the coherent mode-locking pulse. If the coherence relaxation time T_2 is large enough, the polarization waves decay slowly and the modulation amplitude of the induced population gratings increases. Therefore the cavity length imposes restrictions on the time T_2. In our calculations, the regime disappeared when the time T_2 exceeded the round-trip time of the cavity by an order of magnitude.

The gain parameters have not got such rigid restrictions. The media with much longer relaxation times can be used here as compared to the absorber. Specifically, the values of T_{2g} up to ∼100 fs can be exploited. Such values of T_{2g} can be obtained, for instance, in the semiconductor amplifiers.

The cavity length also limits the inversion relaxation time T_1. This limitation is not so strict for a gain as for an absorber, since the pulse is not exactly a 2π pulse and it does not completely return the medium to the ground state. As a result, absorption decreases and for large enough values of the time T_{1a} the absorber ceases to act as a nonlinear coherent loss modulator.

The coherent mode-locking regime requires that the transition dipole moment in the gain medium is being twice more than in the absorber [11]. However, calculations show that deviations are acceptable in the direction of increasing or decreasing this ratio.

Obtained theoretical results arise the question about the choice of the active media for a laser. Our calculations have shown that several restrictions have to be imposed on the active media to enable the stable coherent mode-locking in an ultrashort cavity. Firstly, the absorber has to exhibit extremely small values of the relaxation time T_{2a}. In order of magnitude, it should coincide with the round-trip time taking the light to travel around the ultrashort cavity, i.e., we need $T_{2a} < 100$ fs. Secondly, the inversion relaxation should be fast enough, with the typical values $T_{1a} < 1$ ps. Thirdly, the two- or few-level approximation must be valid for the description of the optical response of the medium.

A number of media can be expected to satisfy these criteria. For example, multiple-quantum-well structures used as the active medium in quantum-cascade lasers can be considered. They typically possess ultrashort relaxation times, with $T_2 < 100$ fs and $T_1 < 1$ ps, while their dynamics is well reproduced by means of a two- or three-level model [41]. Next, metal-insulator structures are known to have extremely fast relaxation times with $T_2 \sim 10$ fs and T_1 of the order of hundreds of femtoseconds [42], i.e., the range of the relaxation parameters used in our numerical calculations. Interband transitions of metal-insulator structures lie in the optical and adjacent frequency ranges. We should note that the self-induced transparency in the metal-dielectric structures was investigated theoretically [42] and it was shown that the pulses with the duration of several femtoseconds could propagate without significant losses. Besides, semiconductor quantum dots can also be exploited. Quantum dots naturally possess a discrete energy level structure, which allows to describe their response with few-level models. They were also shown to exhibit not only fast coherence relaxation with the possibility of $T_2 < 100$ fs but also largely enhanced carrier relaxation rate as compared to bulk semiconductors with subpicosecond effective values of T_1 [43,44]. Finally, it is also possible that the practical implementation of an ultrashort laser operating in the coherent mode-locking regime will require a semiconductor, metal, and dielectric combination. Such a combination will provide the required ratio of dipole moments and values of the relaxation times and concentrations.

For the parameters we considered above, the peak intensity is $\approx$0.6 TW/cm^2. Since the laser is small in the longitudinal dimension, its transverse dimensions can be also very small, facilitating a possibility of a straightforward on-chip integration. For instance, if we consider a device with just a 10 μm diameter, this would give us consequently $\approx$0.5 nJ pulse energy. We note also that the nature of the coherent mode-locking (and in particular the fact that the pulse duration is smaller than the coherence times) immediately ensures that the pump energy obtained by the laser is fully radiated into the laser pulse, while the energy dissipation in the nonradiative channels such as heat is expected to be negligible.

It is also important to address the validity of the two-level model in the consideration above. Indeed, the near single-cycle duration of the obtained pulse in Fig. 4 and its ultrabroad spectrum make the two-level approximation inapplicable for the detailed modeling of the pulse interaction with the active medium. However, Rabi flopping with few-cycle optical pulses was observed in multiple experiments, even in such complex media as semiconductors [26,41,45]. It is worth to mention therefore that there is no fundamental limit on the temporal duration of Rabi oscillations.

Moreover, a number of theoretical studies of the propagation of extremely short self-induced transparency solitons in multilevel media were performed [46–49], which showed that the resulting dynamics can be qualitatively well described using a simple two-level model. Hence, we can expect the obtained above dynamics to show up as well in active media with more complex energy level structure.

IV. SCALING RULES

Finally, it seems interesting to look for a way to decrease the duration of the generated single-cycle pulse. Therefore we are interested to check the equations (1)–(6) for scaling rules, which would allow rescaling obtained above solutions to even shorter pulse durations. To start with, we assume that all time quantities in our system are rescaled by a factor K:

$$t \to t/K, \qquad T_1 \to T_1/K, \quad T_2 \to T_2/K, \\ \omega_0 \to \omega_0 K, \quad \gamma \to \gamma K, \tag{7}$$

which implies the compression of the duration of the generated pulse in K times. From Eq. (1), it now directly follows that the spatial coordinates have to be rescaled accordingly:

$$z \to z/K, \tag{8}$$

i.e., the lengths of all intracavity elements, including the length of the whole cavity, are to be also reduced in K times. The physical meaning of the density matrix elements ρ_{12} and n requires them to remain unchanged together with the equilibrium value n_0:

$$\rho_{12}, n, n_0 = \text{const.} \tag{9}$$

Now from Eqs. (1)–(4), one can find the rescaling for the quantities E, P, d_{12}, and N_0. It is important to notice, that several scaling rules can be devised for these quantities. We would be particularly interested to keep the transition dipole moment d_{12} constant, since it is in general much harder to vary it as compared, for instance, to the density of particles N_0. Now one readily gets from Eqs. (1)–(4):

$$E \to E\,K, \quad P \to P\,K, \\ N_0 \to N_0\,K, \quad d_{12} = \text{const.} \tag{10}$$

Finally, for the quantities describing the metallic cavity mirrors, we find from Eqs. (5) and (6):

$$E \to E\,K, \quad x \to x/K, \\ P \to P\,K, \quad N_{el} \to N_{el}\,K^2. \tag{11}$$

As already stated above, other scaling rules for quantities (10) also exist with the prescribed scalings (7)–(9). For example, we can derive the following scaling rule, which holds the density of particles N_0 constant:

$$E \to E\,\sqrt{K}, \quad P \to P\,\sqrt{K}, \\ N_0 = \text{const}, \quad d_{12} \to d_{12}\,\sqrt{K}. \tag{12}$$

When dealing with few-cycle or even shorter pulses the relaxation times T_1, T_2, and γ^{-1} can be safely assumed to be very large, meaning that all relaxation terms in Eqs. (1)–(6) can be neglected. Therefore the scaling of T_1, T_2, and γ^{-1} does not in fact play any role. Hence, the compression of the generated pulse is provided by the scaling of the medium parameters $\omega_0, d_{12},$ and N_0. The density of particles N_0 can be varied, for instance, by controlling the pressure in gaseous media or the doping concentration in doped solids with rear-earth ions. At the same time, the parameters ω_0 and d_{12} in such media can not be varied by design, so one can only rely on changing the resonant medium itself. At the same time, parameters ω_0 and d_{12} can be readily tuned in low-dimensional semiconductor structures: quantum wells, quantum dashes, and quantum dots.

For low-dimensional structures of a spatial size L the transition parameters scale as

$$\omega_0 \sim \frac{1}{L^2}, \quad d_{12} \sim L.$$

For such a case, one can find alternative scaling rule instead of Eqs. (10) and (12):

$$\begin{aligned} E &\to E\,K^{3/2}, \quad P \to P\,K^{3/2}, \\ N_0 &= N_0\,K^2, \quad d_{12} \to d_{12}/\sqrt{K}, \end{aligned} \tag{13}$$

where the scaling factor is $K = L^{-2}$.

V. CONCLUSIONS

In conclusion, we have theoretically shown that in a two-section laser with an ultrashort cavity it is possible to obtain the coherent mode-locking with the self-induced transparency pulse containing several or even one optical cycles. In this case, the pulse repetition rate falls into the terahertz range. This regime is self-starting and does not require any external seed pulse, which is extremely important for the practice.

Besides that, we have also derived a number of scaling rules, which enable obtaining even shorter pulses in ultrashort-cavity lasers, if the optical parameters of the gain and absorber media are accordingly rescaled. We believe that our findings provide a noticeable step towards the development of ultracompact laser sources of few- and single-cycle pulses.

ACKNOWLEDGMENTS

R.A., A.P., and N.R. thanks the financial support from Russian Science Foundation, Project 21-72-10028. I.B. acknowledges support from Deutsche Forschungsgemeinschaft (DFG, German Research Foundation), projects BA 4156/4-2 as well as from Germany's Excellence Strategy within the Cluster of Excellence PhoenixD (EXC 2122, Project ID 390833453).

[1] U. Keller, Nature (London) **424**, 831 (2003).
[2] U. Keller, Appl. Phys. B **100**, 15 (2010).
[3] E. Rafailov, M. Cataluna, and W. Sibbett, Nat. Photon. **1**, 395 (2007).
[4] J. C. Diels and W. Rudolph, *Ultrashort Laser Pulse Phenomena* (Elsevier, Amsterdam, 2006).
[5] U. Morgner, F. X. Kärtner, S. H. Cho, Y. Chen, H. A. Haus, J. G. Fujimoto, E. P. Ippen, V. Scheuer, G. Angelow, and T. Tschudi, Opt. Lett. **24**, 411 (1999).
[6] Y. Song, Z. Wang, C. Wang, K. Panajotov, and H. Zhang, Adv. Photon. **2**, 024001 (2020).
[7] Y. Han, Y. Guo, B. Gao, C. Ma, R. Zhang, and H. Zhang, Prog. Quant. Elect. **71**, 100264 (2020).
[8] J. Liu, J. Wu, H. Chen, Y. Chen, Z. Wang, C. Ma, and H. Zhang, Sci. Chin. Phys. Mech. Astr. **64**, 1 (2021).
[9] P. G. Kryukov and V. Letokhov, Sov. Phys. Usp. **12**, 641 (1970).
[10] L. Allen and J. H. Eberly, *Optical Resonance and Two-Level Atoms* (Wiley, New York, London, 1975).
[11] V. V. Kozlov, Phys. Rev. A **56**, 1607 (1997).
[12] V. P. Kalosha, M. Müller, and J. Herrmann, Opt. Lett. **23**, 117 (1998).
[13] V. P. Kalosha, M. Müller, and J. Herrmann, J. Opt. Soc. Am. B **16**, 323 (1999).
[14] C. R. Menyuk and M. A. Talukder, Phys. Rev. Lett. **102**, 023903 (2009).
[15] M. A. Talukder and C. R. Menyuk, Phys. Rev. A **79**, 063841 (2009).
[16] V. V. Kozlov, N. N. Rosanov, and S. Wabnitz, Phys. Rev. A **84**, 053810 (2011).
[17] V. V. Kozlov and N. N. Rosanov, Phys. Rev. A **87**, 043836 (2013).
[18] R. Arkhipov, M. Arkhipov, and I. Babushkin, JETP Lett. **101**, 149 (2015).
[19] R. Arkhipov, M. Arkhipov, and I. Babushkin, Opt. Commun. **361**, 73 (2014).
[20] R. M. Arkhipov, M. V. Arkhipov, I. Babushkin, and N. N. Rosanov, Opt. Lett. **41**, 737 (2016).
[21] R. M. Arkhipov, A. V. Pakhomov, M. V. Arkhipov, I. V. Babushkin, and N. N. Rosanov, Sci. Rep. **11**, 1147 (2021).
[22] S. L. McCall and E. L. Hahn, Phys. Rev. Lett. **18**, 908 (1967).
[23] S. L. McCall and E. L. Hahn, Phys. Rev. **183**, 457 (1969).
[24] I. A. Poluektov, Y. M. Popov, and V. S. Roytberg, Sov. Phys. Usp. **17**, 673 (1975).
[25] P. Borri, W. Langbein, S. Schneider, U. Woggon, R. L. Sellin, D. Ouyang, and D. Bimberg, Phys. Rev. B **66**, 081306(R) (2002).
[26] O. D. Mücke, T. Tritschler, M. Wegener, U. Morgner, and F. X. Kärtner, Phys. Rev. Lett. **87**, 057401 (2001).
[27] M. Jütte and W. Von der Osten, Journ. Lumin. **83**, 77 (1999).
[28] M. Kolarczik, N. Owschimikow, J. Korn, B. Lingnau, Y. Kaptan, D. Bimberg, E. Schöll, K. Lüdge, and U. Woggon, Nat. Commun. **4**, 2953 (2013).
[29] O. Karni, A. Capua, G. Eisenstein, V. Sichkovskyi, V. Ivanov, and J. P. Reithmaier, Opt. Expr. **21**, 26786 (2013).
[30] N. N. Rosanov, I. A. Aleksandrov, M. V. Arkhipov, R. M. Arkhipov, I. Babushkin, N. A. Veretenov, A. Dadeko, D. A. Tumakov, and S. V. Fedorov, Quant. Electron. **51**, 959 (2021).
[31] A. Fox and P. Smith, Phys. Rev. Lett. **18**, 826 (1967).
[32] M. Arkhipov, R. Arkhipov, A. Shimko, and I. Babushkin, JETP Lett. **101**, 232 (2015).
[33] M. Arkhipov, A. Shimko, R. Arkhipov, I. Babushkin, A. Kalinichev, A. Demircan, U. Morgner, and N. Rosanov, Las. Phys. Lett. **15**, 075003 (2018).

[34] M. Arkhipov, R. Arkhipov, A. Shimko, I. Babushkin, and N. Rosanov, JETP Lett. **109**, 634 (2019).
[35] M. Arkhipov, R. Arkhipov, A. Shimko, I. Babushkin, and N. Rosanov, J. Phys.: Conf. Ser. **1410**, 012102 (2019).
[36] M. V. Arkhipov, A. A. Shimko, N. N. Rosanov, I. Babushkin, and R. M. Arkhipov, Phys. Rev. A **101**, 013803 (2020).
[37] F. Krausz and M. Ivanov, Rev. Mod. Phys. **81**, 163 (2009).
[38] M. Born and E. Wolf, *Principles of Optics* (Cambridge University Press, Cambridge, UK, 1999).
[39] R. M. Arkhipov, M. V. Arkhipov, I. Babushkin, A. Demircan, U. Morgner, and N. N. Rosanov, Opt. Lett. **41**, 4983 (2016).
[40] R. M. Arkhipov, A. V. Pakhomov, M. V. Arkhipov, I. V. Babushkin, A. Demircan, U. Morgner, and N. N. Rosanov, Sci. Rep. **7**, 12467 (2017).
[41] H. Choi, V.-M. Gkortsas, L. Diehl, D. Bour, S. Corzine, J. Zhu, G. Hoefler, F. Capasso, F. Kärtner, and T. Norris, Nat. Photon. **4**, 706 (2010).
[42] A. Marini and F. Biancalana, Phys. Rev. Lett. **110**, 243901 (2013).
[43] T. Erneux, E. A. Viktorov, and P. Mandel, Phys. Rev. A **76**, 023819 (2007).
[44] T. Erneux, E. A. Viktorov, B. Kelleher, D. Goulding, S. P. Hegarty, and G. Huyet, Opt. Lett. **35**, 937 (2010).
[45] M. Wegener, *Extreme Nonlinear Optics* (Springer Verlag, Berlin, Heidelberg, New York, 2005).
[46] A. Parkhomenko and S. Sazonov, J. Exp. Theor. Phys. **87**, 864 (1998).
[47] N. Vysotina, N. Rosanov, and V. Semenov, JETP Lett. **83**, 279 (2006).
[48] N. V. Vysotina, N. N. Rosanov, and V. E. Semenov, Opt. Spectr. **106**, 713 (2009).
[49] N. Rosanov, V. Semenov, and N. Vysotina, Quant. Electron. **38**, 137 (2008).

Correction: The previously published images for Figures 6 and 7 were transposed and have been set correctly.